SI Material and Methods

DNA constructs

SET/TAF-Iβ gene was inserted into the pET28a(+) bacterial expression vector, along with an N-terminal His-tag. DNA for cloning was obtained via polymerase chain reaction (PCR) using a cDNAs sequence (Geneservice, UK). The oligonucleotides used in the PCR to amplify the DNA encoding SET/TAF-Iβ were 5'-agccatatgatgtcggcgccggcggcc-3' and 5'-gtgctcgagttagtcatcttctccttc-3'. The DNA encoding for C*c* was already in the pBTR1 vector (1, 2), along with yeast heme lyase for proper heme folding. DNAs encoding for core histones from *Xenopus laevis* were in the pET3a vector obtained from Dr Tim Richmond (Institute of Molecular Biology and Biophysics, Switzerland). SET/TAF-$I\beta_{(1-80)}$ (amino acids 1-80) and SET/TAF-$I\beta_{(81-277)}$ (amino acids 81-277) were cloned into the pET28a(+) vector. For PCR amplification of the two last coding DNA sequences, primers 5'-agccatatgatgtcggcgccggcggcc-3' and 5'-gtgctcgagttaatttgggattttggc-3' were used SET/TAF-$I\beta_{(1-80)}$, while oligonucleotides 5'-agccatatgttttgggtaacaacattt-3' and 5'-gtgctcgagttagtcatcttctccttc-3' were used for SET/TAF-$I\beta_{(81-277)}$. SET/TAF-Iβ triple mutants S162A/K164A/D165A and T191A/T194A/D195A were available in the pET14b expression vector provided by Dr Masami Horikoshi (University of Tokyo, Japan). Constructs were confirmed through automated sequencing.

Antibodies

Rabbit anti-human C*c* serum was obtained after immunizing male rabbits with full-length recombinant C*c* suspended in a 0.85% solution of NaCl (20 mg/ml). The suspension was then incorporated into an equal amount of complete (Freund) adjuvant obtained from Difco (BD Biosciences, US). Mouse monoclonal anti-α-Tub (catalog number T8328), as well as secondary horseradish peroxidase (HRP)-conjugated anti-mouse IgG (catalog number A4416) and anti-rabbit IgG (catalog number A0545) were obtained from Sigma-Aldrich. Rabbit polyclonal antibody to COX IV (anti-COX IV) was from Abcam (catalog number ab16056). Anti-PARP mouse monoclonal antibody (catalog

number 556362) was from BD Pharmingen (BD Biosciences, US). Mouse monoclonal anti-SET/TAF-Iβ was obtained from Calbiochem (catalog number AP1134). Primary mouse anti-γ-H2AX antibody (catalog number 05-636) and secondary goat anti-mouse light chain antibody-HRP conjugate (catalog number AP200P) were acquired from EMD Millipore. Mouse anti-procaspase-3 antibody was from Santa Cruz Biotechnology (catalog number SC-47724) and rabbit anti-cleaved caspase-3 antibody was obtained from Cell Signaling Technology (catalog number 9664).

Cell culture and apoptosis induction

Heltog cells were cultured in Dulbecco's modified Eagle's medium supplemented with 10% heat-inactivated fetal bovine serum, 2 mM L-glutamine, 100 U/ml penicillin, 100 μg/ml streptomycin, and maintained at 37 °C in a humidified 5% CO_2 atmosphere. For subcellular localization of C*c*-GFP, 75,000 Heltog cells were grown on glass slides in a 12-well plate for 48 h and cells were treated with 20 μM CPT (Sigma-Aldrich). After 4 hours nuclei were stained with 1μg/ml Hoechst and, afterwards, cells were fixed in 4% paraformaldehyde in PBS (phosphate buffer saline) for 10 minutes and washed in PBS. The fluorescence of the GFP and Hoechst was detected by confocal microscopy in a Leica TCS-SP5 laser microscope. For subcellular fractioning and IP, 6 x 10^6 Heltog cells were seeded in 140 mm Petri dishes and treated with different apoptosis-inducing agents (20 μM CPT, 20 μM indotecan, 2 μM doxorubicin, 100 ng/ml recombinant TRAIL or 1 μM STP) for the indicated incubation times. Recombinant human TRAIL (residues 95–281) was produced as described previously (3).

Subcellular fractionation

Following detachment with trypsin and prior to fractionation, cells were washed with PBS. Separation of cells into cytosol, membrane/organelle, nucleus and cytoskeleton fractions was performed using a ProteoExtract Subcellular Proteome Extraction Kit (Calbiochem) and following the manufacturer's indications. The purity of the subcellular fractions obtained was verified by

Western blot analysis, using anti-α-Tub, anti-COX IV and anti-PARP for detecting cytosol-, mitochondria- and nucleus-specific proteins, respectively.

Western blot analysis

For the immunoblot detection of C*c*, α-tub, COX IV, PARP and SET/TAF-Iβ in the subcellular fractions or IP samples, protein content was measured using the DC^{TM} protein assay (Bio-Rad Laboratories, US). For the immunodetection of γ-H2AX, procaspase-3 and cleaved caspase-3, total lysates were obtained after the addition of PBS buffer supplemented with protease inhibitors and sonication, followed by protein content detection with the DC Protein Assay (Bio-Rad, 20 μg protein was loaded onto each lane). Proteins were resolved by sodium dodecyl sulphate-polyacrylamide gel electrophoresis (SDS-PAGE) in 12% gels and then transferred onto polyvinylidene fluoride (PVDF) membranes (EMD Millipore) using a Mini Trans-Blot electrophoretic transfer cell (Bio-Rad). Membranes were blocked in 5% nonfat dry milk in PBS with Tween-20 (TPBS) and immunoblot was performed with primary antibodies. HRP-conjugated secondary antibodies were used for detection. The immunoreactive bands were detected using Amersham ECL Plus Western Blotting Detection Reagents (GE Healthcare Life Sciences).

Immunoprecipitation

Cell fractions of nuclei from subcellular fractionation of control and CPT-treated Heltog cells were used for IP. For this, nuclear samples (300 μg protein) were incubated with 50 μl Sepharose 6B (Sigma-Aldrich) for 3 h at 4 ºC under rotation as a pre-clearing step to reduce nonspecific binding. For C*c* IP, lysates were then centrifuged and 20 μl rabbit anti-human C*c* were added to supernatants and incubated overnight at 4 ºC under rotation. For reverse IP, 1μg SET/TAF-Iβ antibody was added to supernatants and incubated in the same conditions as before. As a negative control, 300 μg nuclear lysates were incubated with 1 μg anti-mouse IgG under the same conditions. Subsequently, 50 μl Protein A Sepharose (GE Healthcare) was added to each lysate for 4 h at 4 ºC under rotation. The protein-sepharose complexes were washed extensively, collected by centrifugation and boiled in freshly prepared reducing

loading buffer. Controls including 30 μg nuclear lysates were run concurrently with the IP samples in the Western blot assays.

Protein expression and purification

C*c* was expressed in *E. coli* BL21(DE3) strains. For this, 25 ml of overnight pre-cultures were shaken at 37 ºC in Luria-Bertani (LB) medium supplemented with 100 μg/ml ampicillin. 2.5 ml of pre-culture was used to inoculate 2.5 l of the same media in a 5 l Erlenmeyer flask. The culture was shaken at 30 ºC for 24 h, after which the cells were harvested at 6,000 rpm for 10 min using an Avanti J-25 refrigerated centrifuge (Beckman Coulter, US). Then, cells were resuspended in 1.5 mM borate buffer solution at pH 8.5, sonicated for 4 min and then centrifuged at 20,000 rpm for 20 min. 1 l of saturated C*c* culture yielded 15 ml of lysate. For NMR measurements, ^{15}N-labeled C*c* was produced in minimal media with $^{15}NH_4Cl$ as nitrogen source. Further purification of C*c* was carried out as indicated in previous studies (2, 4). The fractions containing C*c* were concentrated in Amicon (3 kDa cut-off) until reaching the appropriate C*c* concentration and dialyzed against 10 mM sodium phosphate at pH 7.4 for EMSA and ITC measurements. For NMR titrations, C*c* was dialyzed against 5 mM sodium phosphate at pH 6.3, both in the presence and in the absence of 100 mM KCl.

Constructs containing *wild-type* SET/TAF-Iβ, SET/TAF-I$\beta_{(1\text{-}80)}$, SET/TAF-I$\beta_{(81\text{-}277)}$, and mutants S162A/K164A/D165A and T191A/T194AD195A were used to transform *E. coli* BL21(DE3) strains. Transformed cells were harvested in fresh plates with 50 μg/ml kanamycin at 37 ºC. 250 ml pre-cultures in LB medium supplemented with kanamycin were grown overnight and then used to inoculate 2.5-l cultures in 5-l flasks. After induction of cultures (1 mM isopropyl β-D-1-thiogalactopyranoside [IPTG]) and growth at 30 ºC for 24 h, the cells were harvested at 6,000 rpm for 10 min and resuspended in 40 ml lysis buffer composed of 20 mM Tris-HCl buffer (pH 8), 0.8 M NaCl, 10 mM imidazole, 0.01% phenylmethylsulphonyl fluoride (PMSF), 0.2 mg/ml lysozyme, 5 mM dithiothreitol (DTT) and 0.02 mg/ml DNase. They were then sonicated for 4 min and centrifuged at 20,000 rpm for 20 min. Protein purification was assessed by affinity chromatography. The above lysates were loaded into Ni Sepharose 6

Fast Flow (GE Healthcare) having been previously equilibrated in the above mentioned buffer. Proteins were then eluted by applying an imidazole gradient from 0 to 300 mM. The fractions containing protein were concentrated in Amicon (10 kDa cut-off) until reaching a proper protein concentration and dialyzed against 10 mM sodium phosphate at pH 7.4 for EMSA and ITC measurements or 5 mM sodium phosphate at pH 6.5 for NMR titrations. In all cases, protein solutions contained 0.01% PMSF. Purity of proteins was verified by SDS-PAGE.

Xenopus laevis core histones H2B, H3 and H4 were expressed in BL21(DE3) *E. coli* strains. Constructs containing core histones were used to transform cells, which were plated in LB medium supplemented with 100 μg/ml ampicillin. Single colonies were employed to inoculate 25 ml pre-cultures and incubated for 12 h at 37 ºC. Following induction with 0.5 mM IPTG, cells were grown for 4 h at 25 °C in 5 l LB medium. Purification of core histones was performed as previously indicated (5).

Protein quantification was assessed using the Bradford protein assay (6) and the SET/TAF-Iβ protein concentration was expressed in dimeric form.

EMSA

SET/TAF-Iβ (5 μg) was mixed with 2.5 μg calf thymus histones (Sigma-Aldrich) and/or C*c* (0.5-8 μg) in 20 μl of 10 mM sodium phosphate at pH 7.4, incubated for 30 min at room temperature and analysed on 1% agarose gel in the same buffer at 75 mA for 2 h. Proteins were stained with Coomassie Brilliant Blue.

NMR measurements

1D ^{1}H NMR and 2D [^{1}H, ^{15}N] HSQC spectra of C*c* was performed on a Bruker Avance 700 MHz at 25 ºC. Water signal was suppressed according to the WATERGATE solvent suppression method (7). NMR measurements of reduced C*c* were made in 5 mM sodium phosphate buffer pH 6.3 in the presence of 0.1 M sodium ascorbate to ensure the redox state. NMR titrations of oxidized C*c* were performed after oxidizing C*c* with an excess of potassium ferricyanide, followed by extensively washing. To adjust the lock signal, 10% D_2O was

added. The NMR signal assignment of the ^{15}N and ^{1}H nuclei of reduced C*c* (BMRB accession number: 5406) (8) and oxidized C*c* (BMRB 26578) are available.

1D ^{1}H spectra were recorded to monitor the Met-80 methyl signal of reduced C*c* (13 μM) in the presence of 3.5 μM unlabelled SET/TAF-Iβ and *Xenopus laevis* core histones H2B, H3 or H4 (5-40 μg), in 5 mM sodium phosphate buffer pH 6.3. 1D ^{1}H measurements of reduced C*c* (13 μM) were also taken after adding 3.5 μM unlabelled BSA to the same buffer. To avoid non-specific interactions, 1D ^{1}H spectra of reduced C*c* (6 μM) were also recorded in the presence of 15 μM unlabelled SET/TAF-Iβ and histone mixture (10-400 μg) in the same buffer as before containing 100 mM KCl.

The interaction of reduced or oxidized C*c* with SET/TAF-Iβ was followed by acquiring two-dimensional [^{1}H-^{15}N] HSQC spectra during titration of 50 μM ^{15}N-labelled C*c* solutions with amounts of each protein partner increasing to a final C*c*:partner molar ratio of 1:0.25. Titration measurements were prepared in NMR tubes (Shigemi, US) up to a 0.35 ml volume. pH values of the samples were verified after each titration step. Data were processed using TopSpin NRM 2.0 software (Bruker) and CSP analyses were performed with Sparky 3 NMR Assignment Program (T.D. Goddard and D.G. Kneller, University of California – San Francisco, US). In order to discriminate between specific line broadenings, threshold values were fixed at $\Delta\Delta\nu_{1/2\ Binding} \geq 14.6$ Hz for ^{15}N, as previously reported (9).

ITC titrations

All ITC experiments were performed using a MicroCal Auto-iTC200 (Malvern Instruments, UK) at 25 ºC by titrating SET/TAF-Iβ with C*c* or core histones. The reference cell was filled with distilled water. The experiments consisted of 2 μl injections of 300 μM C*c*, H2B, H3 or H4 core histones in 10 mM sodium phosphate buffer (pH 7.4) in the presence or absence of 100 mM KCl into the sample cell, which initially contained 20 μM C*c* protein partner solution – namely, SET/TAF-Iβ, SET/TAF-Iβ$_{(1-80)}$, SET/TAF-Iβ$_{(81-277)}$, S162A/K164A/D165A

or T191A/T194AD195A – in the same buffer. All solutions were degassed before the titrations were performed. Titrant was injected at appropriate time intervals to ensure that the thermal power signal returned to the baseline prior to the following injection. To achieve homogeneous mixing in the cell, the stirring speed was maintained constant at 1,000 rpm. The data – namely, the heat per injection normalized per mole of injectant vs. molar ratio – were analyzed with Origin 7.0 (OriginLab Corp.). Calibration and performance tests of the calorimeter were carried out conducting $CaCl_2$–EDTA titrations with solutions provided by the manufacturer.

Dynamic light scattering (DLS)

DLS assays were performed to evaluate the oligomerization state of the histone mixture (1 mg/ml) in 10 mM sodium phosphate at pH 7.4. DLS experiments were conducted at 25 ºC in a Zetasizer Nano ZS (Malvern Instruments).

CD

CD spectra were recorded in the far-ultraviolet (UV) range (190-250 nm) at 25 ºC on a Jasco J-815 CD spectropolarimeter, (Jasco, US) equipped with a Peltier temperature-control system, using a 1-mm quartz cuvette. Protein concentration was 3 μM in all cases – save for H2B, H3 and H4 (15 μM) – in 10 mM sodium phosphate buffer at pH 7.4. For each sample, an average of 20 scans was made.

Nucleosome assembly assay

As described in an earlier study (10), histone chaperone activity was performed. 0.1 pmol of the closed circular form of pBlueScript II SK(-) plasmid (3 kbp) was relaxed by pre-incubation with 2.5 U wheat germ Topo I (Promega, US) in 50 μlTopo buffer consisting of 10 mM Tris-HCl (pH 8), 100 mM NaCl, 3.5 mM $MgCl_2$, 0.5 mM DTT, 2 mM adenosine triphosphate (ATP) and 0.1 mg/ml bovine serum albumin (BSA) at 37 ºC for 3 h. The pBlueScript II SK(-) plasmid was purified by classical plasmid DNA minipreparation using alkaline lysis described elsewhere. 3 pmol of HeLa core histones (EMD Millipore) were pre-incubated with 4 pmol SET/TAF-Iβ in 50 μl assembly buffer composed of 10 mM Tris-HCl

(pH 8), 100 mM NaCl, 2 mM $MgCl_2$, 0.5 mM DTT, 2 mM ATP and 0.1 mg/ml BSA) at 37 ºC for 3 h. When indicated, C*c* (0.5-2 μg) was added to the histone-chaperone mixture. Histone-chaperone samples (with or without C*c*) were then mixed with the relaxed form of plasmid and further incubated at 37 ºC for 3 h. The reactions were stopped by adding equal volume of stop buffer composed of 20 mM EDTA (pH 8), 1% SDS and 0.2 mg/ml proteinase K and incubated at 37 ºC for 30 min. Following the reaction, plasmids were extracted using phenol-chloroform and precipitated with ethanol. Plasmids were subjected to electrophoresis with 1% agarose gel, run in Tris-borate-EDTA buffer and further visualized by staining with ethidium bromide. Histone chaperone activity is identified through accumulation of negative supercoils introduced in circular DNA by SET/TAF-Iβ due to nucleosome formation.

Molecular docking

A model of SET/TAF-Iβ including the missing loops in the crystallographic structure was created through simulated annealing and using X-ray diffraction data as a template. A soft docking algorithm implemented in the Biomolecular complex Generation with Global Evaluation and Ranking (BiGGER) software package (11) was used to generate *in silico* models of the C*c*:SET/TAF-Iβ complex. For each run, 500 solutions were generated using a 15º angle step soft dock and a distance of 7 Å. Geometric docking solutions were generated based on the complementarity of protein surfaces. These solutions were evaluated and ranked according to their “global score”, taking into account different interaction criteria including electrostatic energy of interaction, relative solvation energy and the relative propensity of side chains to interact. The center of mass for all structures was represented. CSP values were taken from NMR measurements and introduced as restraints in the docking calculations. The coordinates file of C*c* was 1J3S, whereas for SET/TAF-Iβ protein, missing loops in the crystallographic structure (PDB code: 2e50) (12) where modelled by simulated annealing using MODELLER (13). Results were evaluated with the zDOPE score, which ranged from -1.3 to -1.5. All molecular graphics of complexes were generated using the UCSF Chimera package (14).

References

1. Olteanu A, *et al.* (2003) Stability and apoptotic activity of recombinant human cytochrome *c*. *Biochem Biophys Res Commun* 312(3):733-740.
2. Moreno-Beltrán B, *et al*. (2015) Respiratory complexes III and IV can each bind two molecules of cytochrome *c* at low ionic strength. *FEBS Lett* 589(4):476-483.
3. MacFarlane M*, et al.* (1997) Identification and molecular cloning of two novel receptors for the cytotoxic ligand TRAIL. *J Biol Chem* 272(41):25417-25420.
4. Rodríguez-Roldán V*, et al.* (2006) A comparative kinetic analysis of the reactivity of plant, horse, and human respiratory cytochrome *c* towards cytochrome *c* oxidase. *Biochem Biophys Res Commun* 346(3):1108-1113.
5. Luger K, Rechsteiner TJ, Flaus AJ, Waye MMY, Richmond TJ (1997) Characterization of nucleosome core particles containing histone proteins made in bacteria. *J Mol Biol* 272(3):301-311.
6. Bradford MM (1976) A rapid and sensitive method for the quantitation of microgram quantities of protein utilizing the principle of protein-dye binding. *Anal Biochem* 72(1–2):248-254.
7. Piotto M, Saudek V, Sklenář V (1992) Gradient-tailored excitation for single-quantum NMR spectroscopy of aqueous solutions. *J Biomol NMR* 2(6):661-665.
8. Jeng W-Y, Chen C-Y, Chang H-C, Chuang W-J (2002) Expression and characterization of recombinant human cytochrome *c* in *E. coli. J Bioenerg Biomembr* 34(6):423-431.
9. Diaz-Moreno I*, et al.* (2005) NMR analysis of the transient complex between membrane photosystem I and soluble cytochrome c_6. *J Biol Chem* 280(9):7925-7931.
10. Umehara T, Chimura T, Ichikawa N, Horikoshi M (2002) Polyanionic stretch-deleted histone chaperone cia1/Asf1p is functional both *in vivo* and *in vitro*. *Genes Cells* 7(1):59-73.
11. Palma PN, Krippahl L, Wampler JE, Moura JJG (2000) BiGGER: A new (soft) docking algorithm for predicting protein interactions. *Proteins: Struct Funct Bioinf* 39(4):372-384.

12. Muto S*, et al.* (2007) Relationship between the structure of SET/TAF-Iβ/INHAT and its histone chaperone activity. *Proc Natl Acad Sci USA* 104(11):4285-4290.
13. Fiser A, Do RKG, Šali A (2000) Modeling of loops in protein structures. *Protein Sci* 9(9):1753-1773.
14. Pettersen EF*, et al.* (2004) UCSF Chimera—A visualization system for exploratory research and analysis. *J Comput Chem* 25(13):1605-1612.

Fig. S1

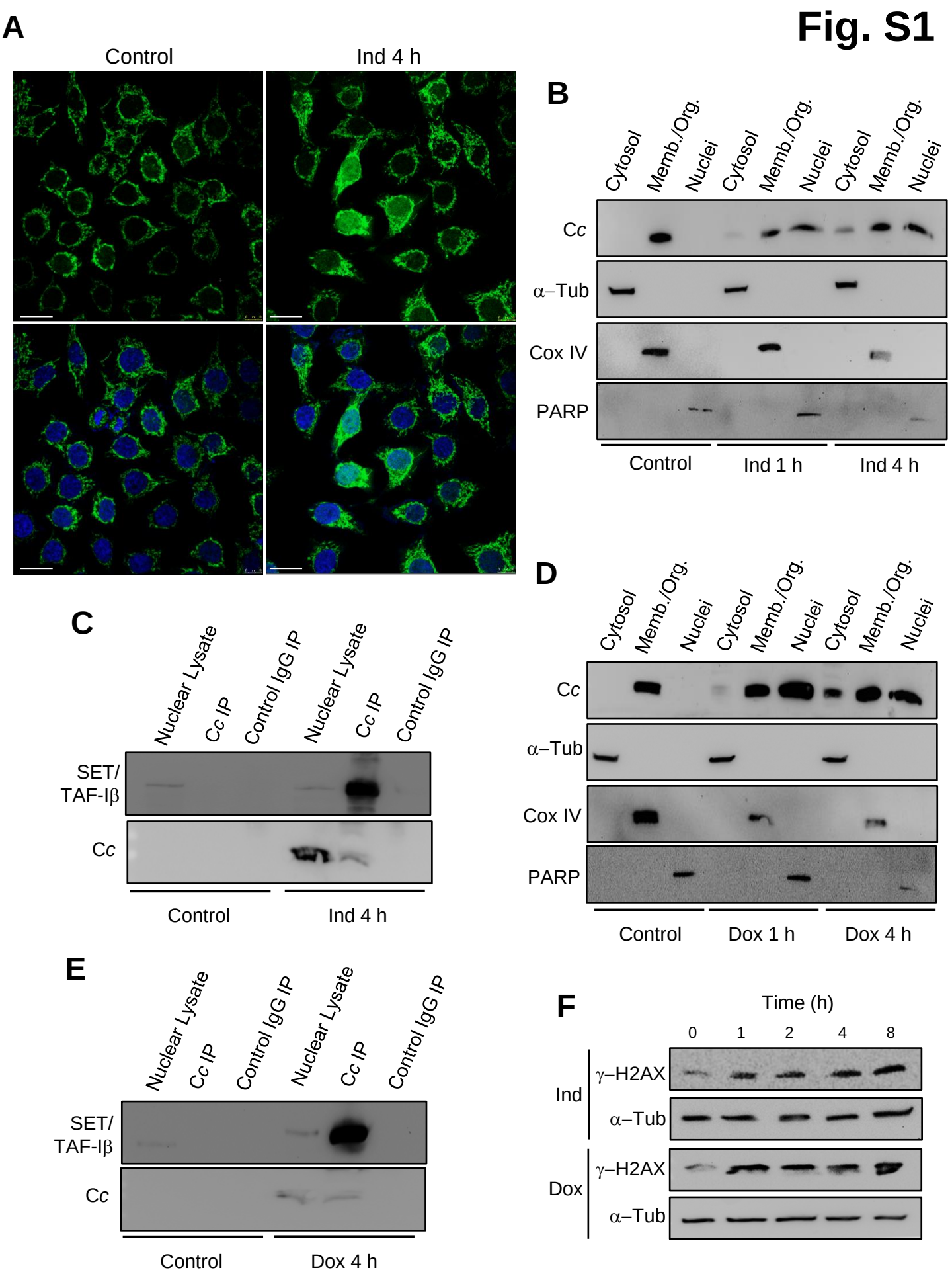
A
Control
Ind 4 h
B
Cytosol
Memb./Org.
Nuclei
Cc
α–Tub
Cox IV
PARP
Control
Ind 1 h
Ind 4 h
C
Nuclear Lysate
Cc IP
Control IgG IP
SET/
TAF-Iβ
Control
Ind 4 h
D
Dox 1 h
Dox 4 h
E
Dox 4 h
F
Time (h)
0
1
2
4
8
Ind
Dox
γ–H2AX

Fig. S2

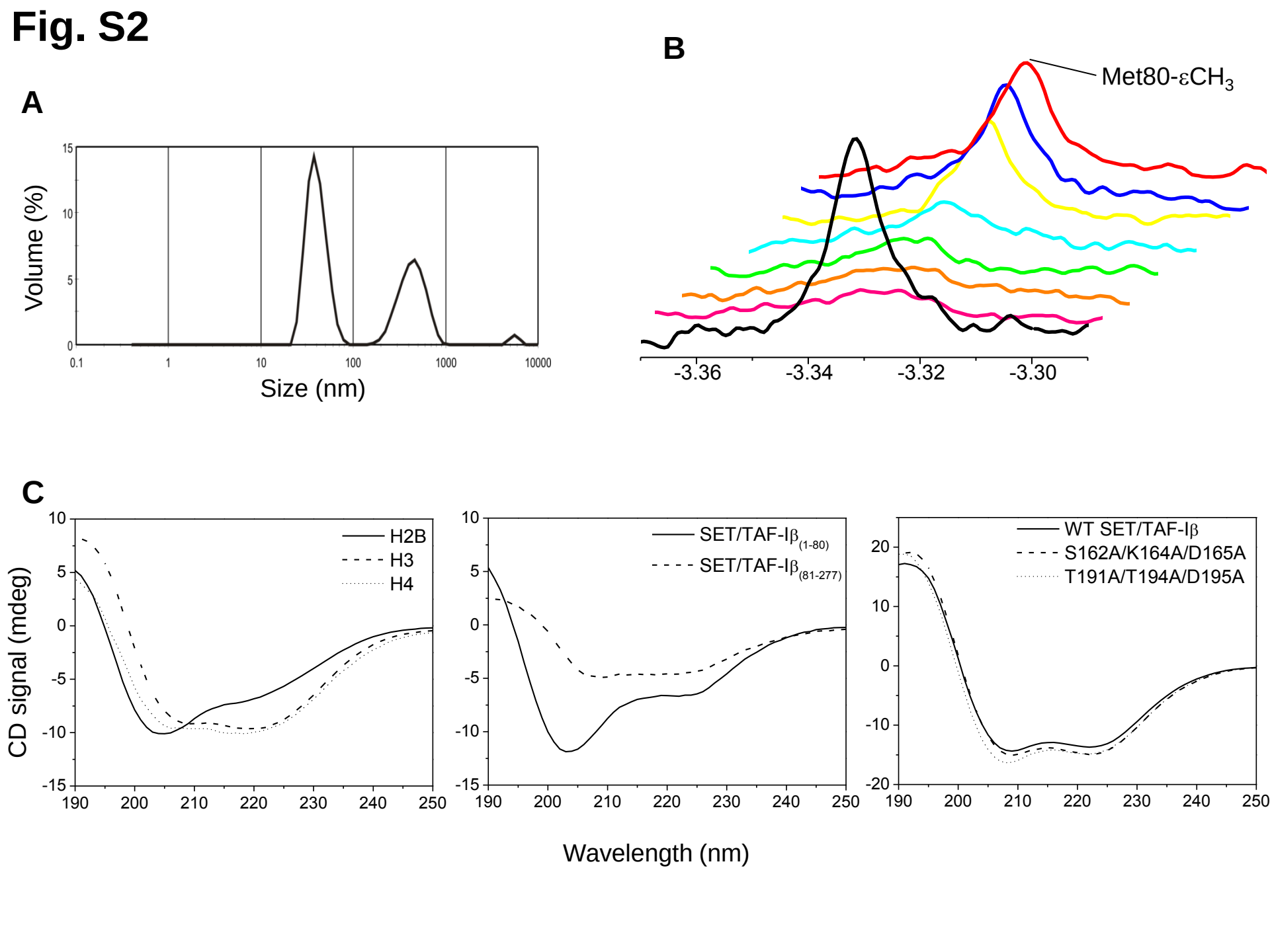
A
Volume (%)
Size (nm)
B
Met80-εCH3
C
CD signal (mdeg)
H2B
H3
H4
SET/TAF-Iβ(1-80)
SET/TAF-Iβ(81-277)
WT SET/TAF-Iβ
S162A/K164A/D165A
T191A/T194A/D195A
Wavelength (nm)

Fig. S3

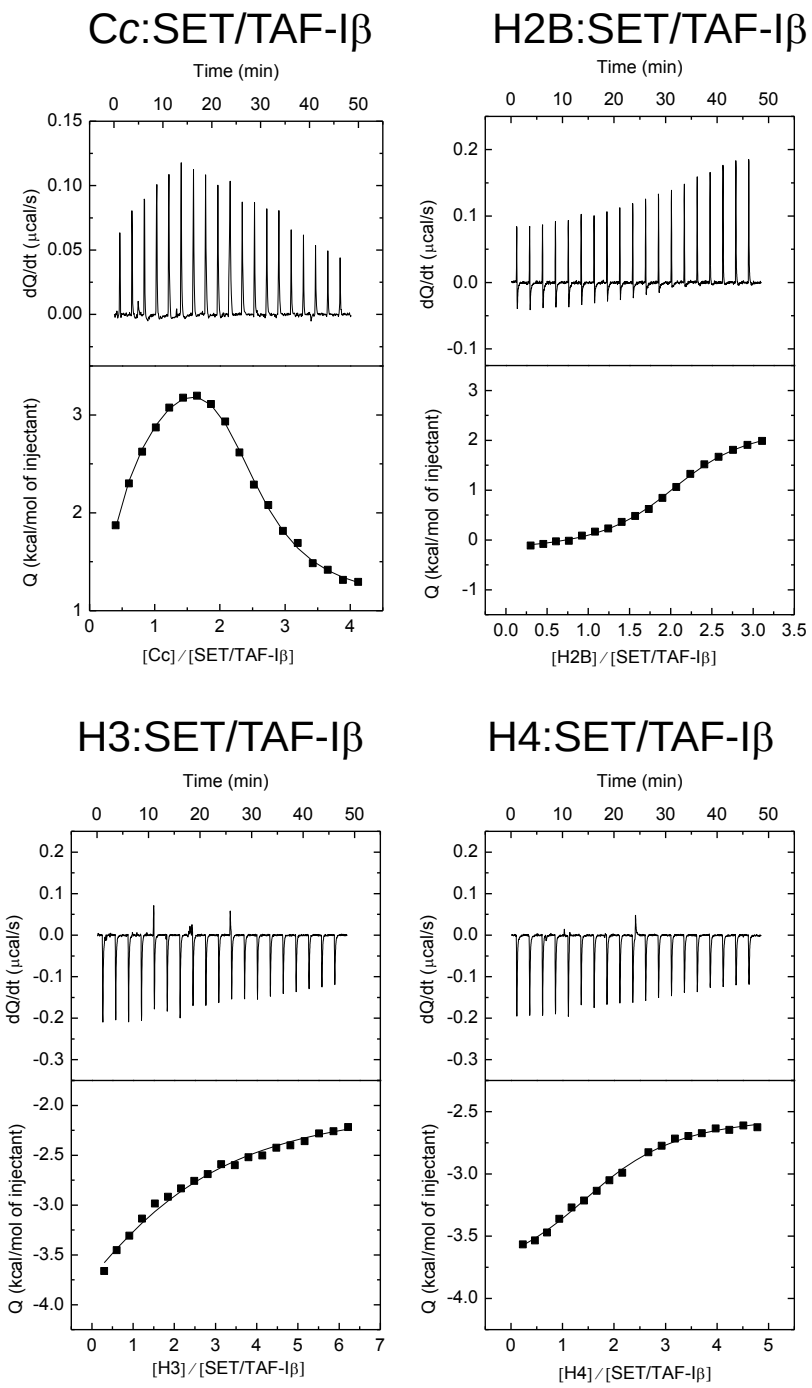
Cc:SET/TAF-Iβ
H2B:SET/TAF-Iβ
H3:SET/TAF-Iβ
H4:SET/TAF-Iβ
Time (min)
dQ/dt (μcal/s)
Q (kcal/mol of injectant)
[Cc]/[SET/TAF-Iβ]
[H2B]/[SET/TAF-Iβ]
[H3]/[SET/TAF-Iβ]
[H4]/[SET/TAF-Iβ]

Figure S4

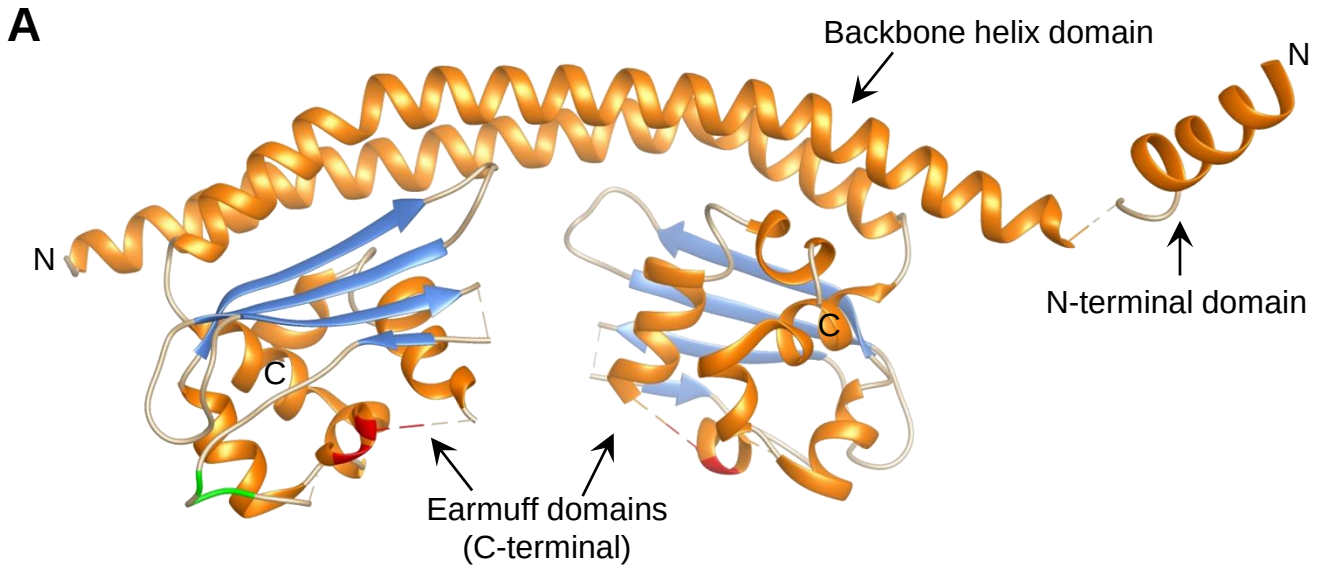

B

```
                                                                                
                                                                                
  1   MSAPAAKVSKKELNSNHDGADETSEKEQQEAIEHIDEVQNEIDRLNEQASEEILKVEQKY  60
                                                                                
                                                                                
 61   NKLRQPFFQKRSELIAKIPNFWVTTFVNHPQVSALLGEEDEEALHYLTRVEVTEFEDIKS 120
                                                                                
                                                                                
121   GYRIDFYFDENPYFENKVLSKEFHLNESGDPSSKSTEIKWKSGKDLTKRSSQTQNKASRK 180
                                                                                
                                                                                
181   RQHEEPESFFTWFTDHS---DAG---ADELGEVIKDDIWPNPLQYYLVPDMDDEEGEGEE  235
                                                                                
                                                                                
236   DDDDDEEEEGLEDIDEEGDEDEGEEDEDDDEGEEGEEDEGEDD  277
```

Figure S5

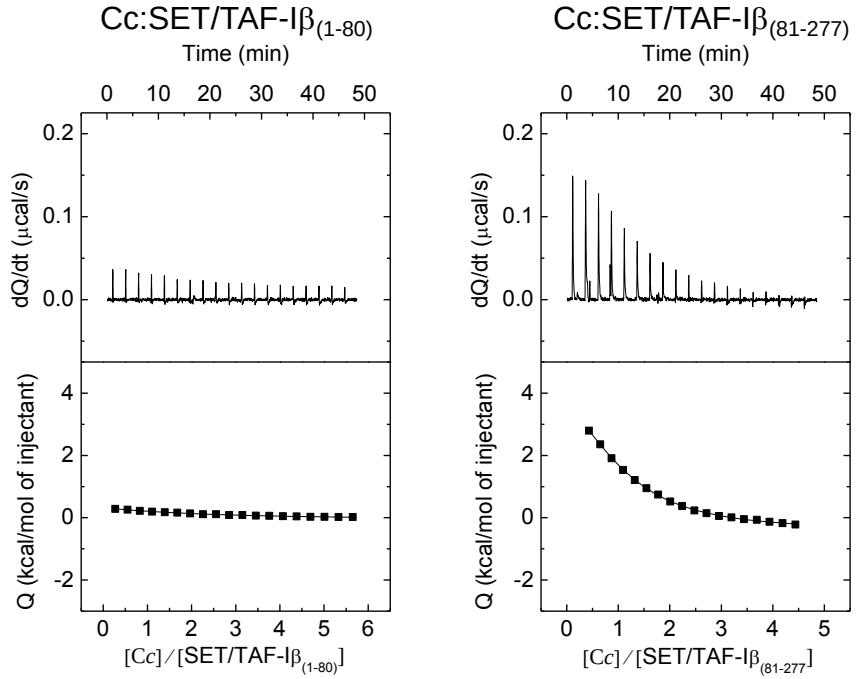
Cc:SET/TAF-Iβ(1-80)
Time (min)
dQ/dt (μcal/s)
Q (kcal/mol of injectant)
[Cc]/[SET/TAF-Iβ(1-80)]

Cc:SET/TAF-Iβ(81-277)
Time (min)
dQ/dt (μcal/s)
Q (kcal/mol of injectant)
[Cc]/[SET/TAF-Iβ(81-277)]

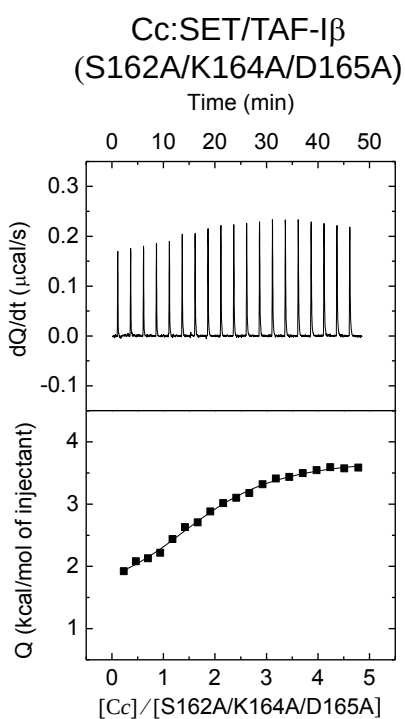
Cc:SET/TAF-Iβ
(S162A/K164A/D165A)
Time (min)
dQ/dt (μcal/s)
Q (kcal/mol of injectant)
[Cc]/[S162A/K164A/D165A]

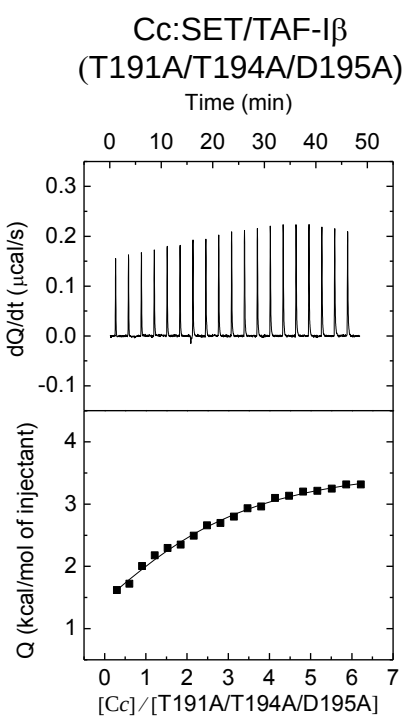
Cc:SET/TAF-Iβ
(T191A/T194A/D195A)
Time (min)
dQ/dt (μcal/s)
Q (kcal/mol of injectant)
[Cc]/[T191A/T194A/D195A]

Figure S6

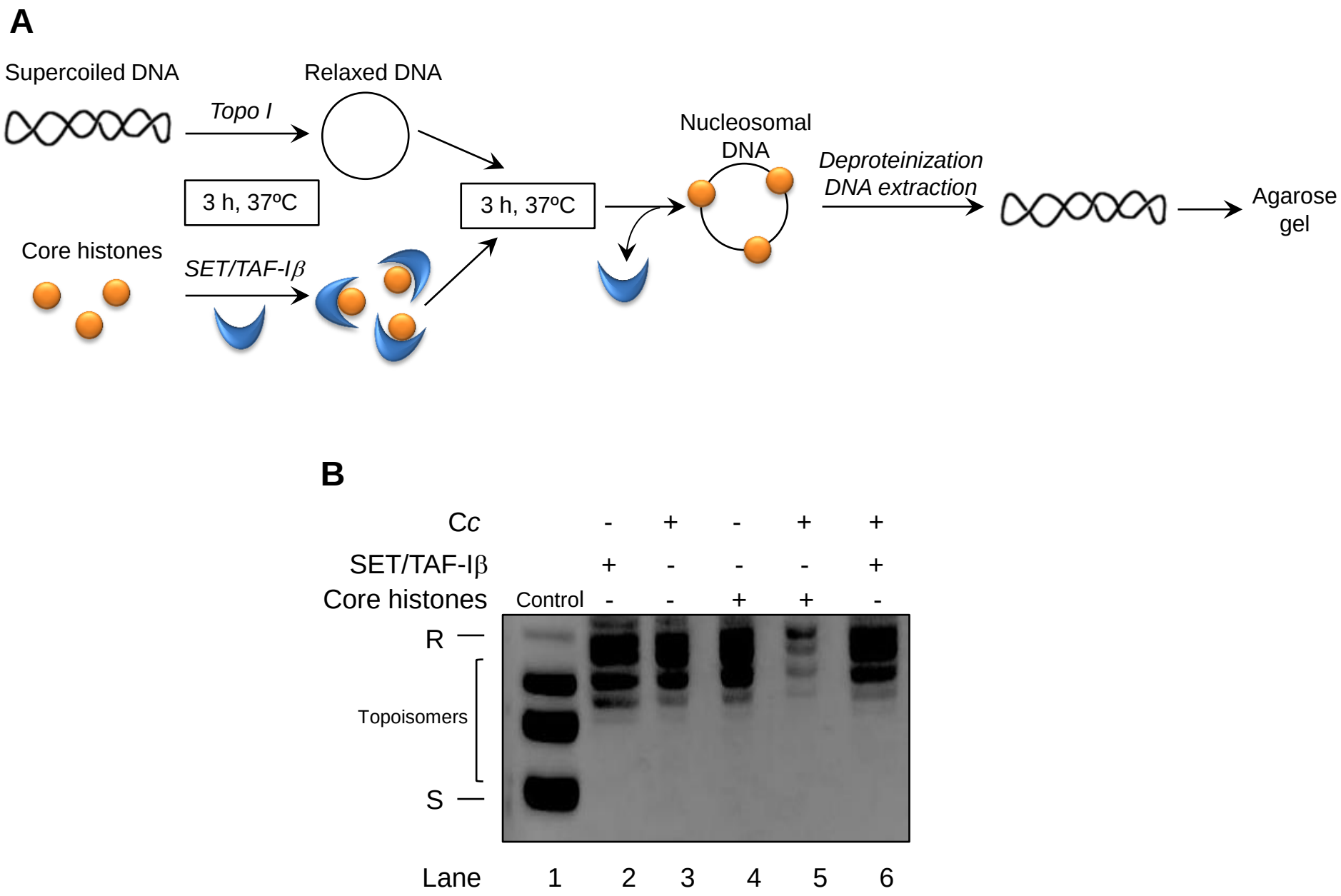
A
Supercoiled DNA
Relaxed DNA
Topo I
3 h, 37ºC
Core histones
SET/TAF-Iβ
3 h, 37ºC
Nucleosomal DNA
Deproteinization DNA extraction
Agarose gel
B
Cc - + - + +
SET/TAF-Iβ + - - - +
Core histones - - + + -
Control
R
Topoisomers
S
Lane 1 2 3 4 5 6

Figure S7

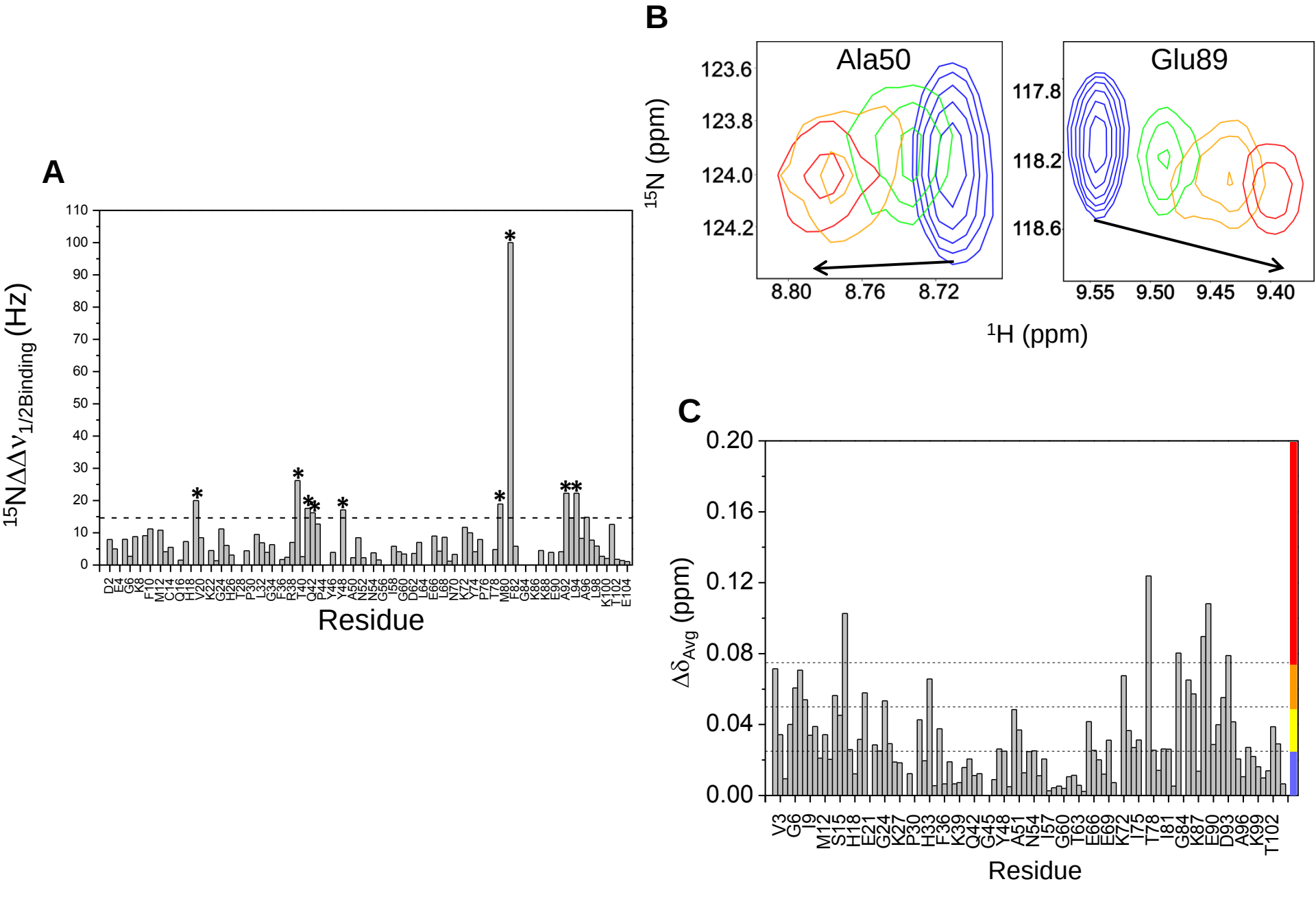
A
$^{15}N\Delta\Delta\nu_{1/2Binding}$ (Hz)
Residue
B
Ala50
Glu89
^{15}N (ppm)
^{1}H (ppm)
C
$\Delta\delta_{Avg}$ (ppm)
Residue

Figure S8

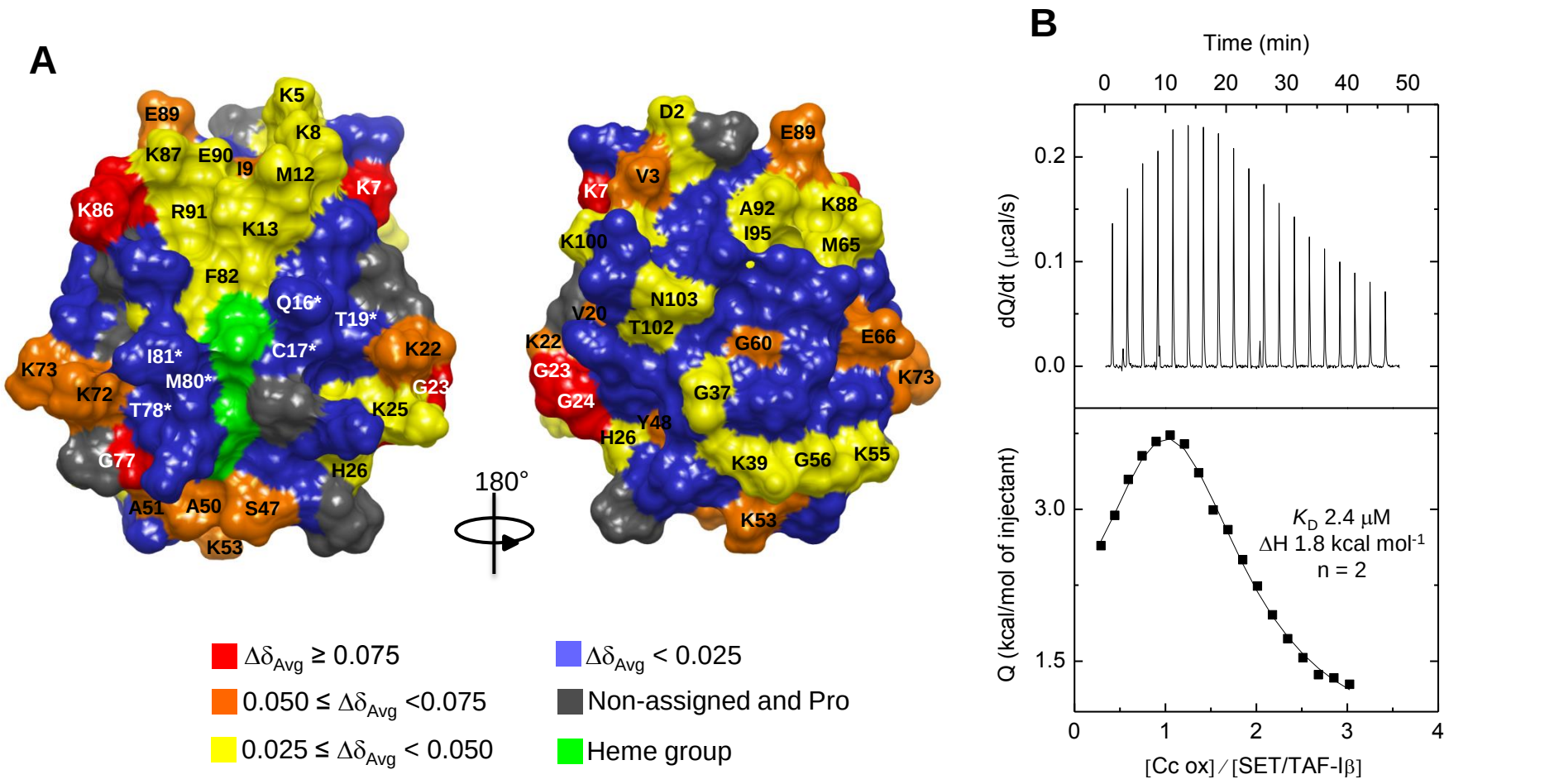
A
K5
E89
K8
K87
E90
I9
M12
K7
K86
R91
K13
F82
Q16*
T19*
I81*
C17*
K22
K73
M80*
G23
K72
T78*
K25
G77
H26
A51
A50
S47
K53
180°
D2
E89
V3
K7
A92
K88
I95
M65
K100
N103
V20
T102
K22
G60
E66
G23
K73
G24
G37
Y48
H26
K39
G56
K55
K53
$\Delta\delta_{Avg} \geq 0.075$
$0.050 \leq \Delta\delta_{Avg} < 0.075$
$0.025 \leq \Delta\delta_{Avg} < 0.050$
$\Delta\delta_{Avg} < 0.025$
Non-assigned and Pro
Heme group
B
Time (min)
0
10
20
30
40
50
0.2
0.1
0.0
dQ/dt (μcal/s)
3.0
1.5
Q (kcal/mol of injectant)
K_D 2.4 μM
ΔH 1.8 kcal mol^{-1}
n = 2
0
1
2
3
4
[Cc ox] / [SET/TAF-Iβ]

Figure S9

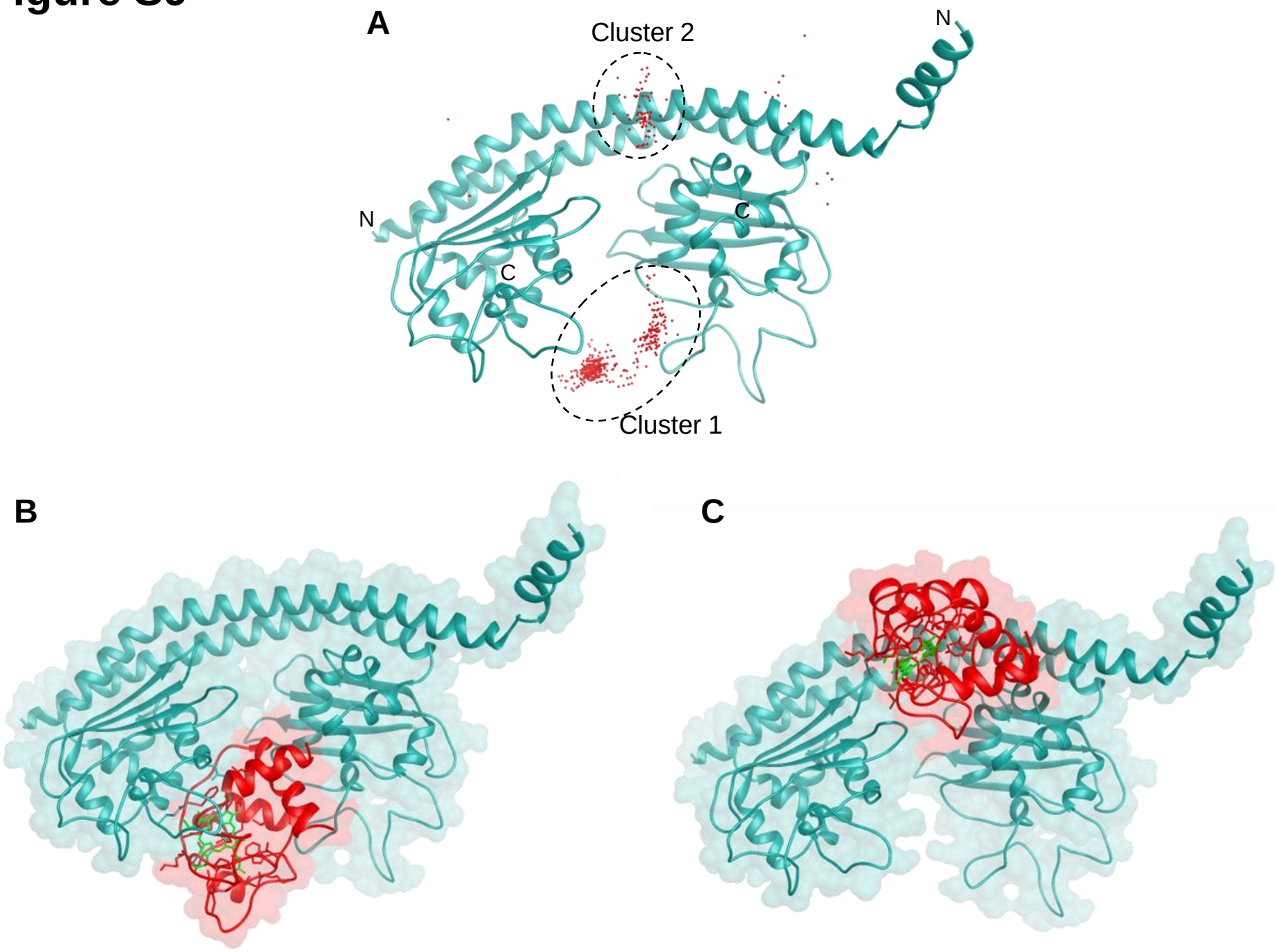

SI Figure Legends

Figure S1. Nuclear translocation of C*c* induced by indotecan (Ind) or doxorubicin (Dox) and formation of the C*c*:SET/TAF-Iβ complex.

(A) Subcellular localization of C*c*-GFP stably expressed (green; upper panel) in Heltog cells upon treatment with 20 μM indotecan for 4 h detected by confocal microscopy (x60 oil objective). Nuclei were stained in blue with Hoechst. Co-localization of green C*c*-GFP fluorescence and blue nuclear staining is shown in the merge images (lower panel). Scale bars are 25 μm.

(B-D) Subcellular fractionation showing endogenous C*c* location following treatment with 20 μM Ind (B) or 2 μM Dox (D) for 1 or 4 h. Untreated and Ind/Dox-treated Heltog cells were fractionated to yield cytosolic, membrane/organelle (Memb./Org.) and nuclear fractions. Purity of subcellular fractions was verified by Western blot using anti-α-Tub (50 kDa), anti-Cox IV (17 kDa) and anti-PARP (116 kDa) antibodies.

(C-E) IP of SET/TAF-Iβ with endogenous C*c* after treatment of Heltog cells with 20 μM Ind (D) or 2 μM Dox (E) for 4 h. Western blot detects SET/TAF-Iβ as a ~34 kDa band (lanes 1 and 4) in the nuclear fraction. C*c* IP of nuclear lysates from untreated (lane 2) and Ind/Dox-treated cells (lane 5), followed by probing with the SET/TAF-Iβ antibody. Confirmation of C*c* IP from nuclear lysates is also shown (lanes 4 and 5) for Ind or Dox treatments.

(F) DNA-damage response following treatment of Heltog cell cultures with 20 μM Ind or 2 μM Dox for 0, 1, 2, 4 and 8 h. Antibody against phosphorylated γ-H2AX was used in Western blots. α–Tub antibody was used as loading control.

Figure S2. (A) DLS profiles showing the oligomerization state of the calf thymus histone mixture at 1 mg/ml. Size distribution is represented against volume. **(B)** 1D ^{1}H NMR spectra showing Met-80 methyl signal of reduced C*c* following addition of SET/TAF-Iβ and histone mixture, in the presence of 100 mM KCl. Details of superimposed 1D ^{1}H NMR spectra of 6 μM reduced C*c* (either free [black] or bound to 15 μM SET/TAF-Iβ [pink]) in presence of histone mixture at increasing

concentrations of 10 μg (orange), 40 μg (green), 100 μg (cyan), 200 μg (yellow), 300 μg (blue) and 400 μg (red). **(C)** Far-UV CD spectra of *Xenopus laevis* core histones H2B, H3 and H4; *wild-type* SET/TAF-Iβ (WT); and mutants SET/TAF-Iβ$_{(1-80)}$, SET/TAF-Iβ$_{(81-277)}$, S162A/K164A/D165A and T191A/T194AD195A.

Figure S3. ITC measurements of SET/TAF-Iβ with C*c* or *Xenopus laevis* core histones H2B, H3 and H4.

Thermograms (upper) and binding isotherms (lower) corresponding to the calorimetric titration with the proteins are shown.

Figure S4. Amino acid sequence and Richardson diagram of SET/TAF-Iβ.

(A) Richardson diagram for overall structure of SET/TAF-Iβ dimer (accession number: 2E50). Residues modified by site-directed mutagenesis in the two triple mutants used in this work are shown in red (T191, T194 and D195) and green (S162, K164 and D165).

(B) Amino acid sequence of SET/TAF-Iβ showing secondary structure elements α-helices (orange) and β-strands (blue). The same color-code as in (A) has been used to highlight mutated residues. Residues in acidic stretch have been underlined.

Figure S5. ITC measurements of C*c* with SET/TAF-Iβ$_{(1-80)}$; SET/TAF-Iβ$_{(81-277)}$, S216A/K164A/D165A and T191A/T194AD195A. The corresponding termograms and binding isotherms (upper and lower, respectively) are shown.

Figure S6. (A) Schematic representation of SET/TAF-Iβ nucleosome assembly activity by means of plasmid supercoiling assays. **(B)** Control experiments for supercoiling assays to determine nucleosome assembly activity of SET/TAF-Iβ. Experimental conditions as indicated in Figure 2D legend. In all lanes, with the exception of lane 1, DNA plasmids were previously treated with Topo I.

Figure S7. NMR titrations of ^{15}N-labeled C*c* with SET/TAF-Iβ.

(A) Differences in line-width ($\Delta\Delta\nu_{1/2Binding}$) in ^{15}N dimension of NMR signals of C*c* amides upon binding to SET/TAF-Iβ. The $\Delta\Delta\nu_{1/2Binding}$ of C*c* amide groups

were calculated from the difference between [^{1}H-^{15}N] HSQC spectra of free C*c* and C*c* in the complex in a C*c*:SET/TAF-Iβ molar ratio of 1:0.25. Residues exhibiting significant line broadening beyond the threshold are marked with an asterisk. The threshold (dashed line) corresponds to the average plus two times the standard deviation ($\Delta\Delta\nu_{1/2Binding} \geq \Delta\Delta\nu_{1/2Binding} + 2S_{n-1}$).

(B) Detail of superimposed [^{1}H-^{15}N] HSQC spectra of free C*c* (blue) and upon titration with increasing SET/TAF-Iβ concentrations at ratios of 1:0.06 (green), 1:0.12 (orange) and 1:0.25 (red). Glu89 and Ala50 resonances correspond to C*c*. Arrows indicate direction and magnitude of CSPs.

(C) The average CSPs ($\Delta\delta_{Avg}$) experienced by amide NMR signals of C*c* in complex with SET/TAF-Iβ, determined at a C*c:* SET/TAF-Iβ ratio of 1:0.25. Color bars represent $\Delta\delta_{Avg}$ categories insignificant (< 0.025 ppm [blue]), small (0.025-0.050 ppm [yellow]), medium (0.050-0.075 ppm [orange]) and large (> 0.075 ppm [red]).

Figure S8. NMR titrations and ITC measurements of oxidized C*c* with SET/TAF-Iβ.

(A) Mapping of oxidized ^{15}N-labeled C*c* residues perturbed following binding to SET/TAF-Iβ. C*c* surfaces have been rotated 180° around a vertical axis in each view. Residues are colored according to their $\Delta\delta_{Avg}$ (ppm). Residues broadened beyond the detection limit are labelled with asterisks.

(B) ITC measurements of oxidized C*c* with SET/TAF-Iβ. The corresponding thermograms and binding isotherms (upper and lower, respectively) are shown. The insert shows the value of the dissociation constant (K_D), associated enthalpy (ΔH) and stoichiometry (n).

Figure S9. NMR-based BiGGER molecular docking of C*c*:SET/TAF-Iβ complex.

(A) Best 500 solutions of NMR-restrained docking for C*c*:SET/TAF-Iβ complex. Mass centers of C*c* are represented by red spheres, while ribbon representation of SET/TAF-Iβ is in cyan.

(B) Transparent surface and ribbon representation for best model at cluster 1 according to global score.

(C) Transparent surface and ribbon representation as in (B) for best model at cluster 2.

Table S1. Thermodynamic values inferred from ITC measurements.

Thermodynamic equilibrium parameters for the interaction of *wild-type* and mutant SET/TAF-Iβ with reduced C*c,* H2B, H3 or H4 core histones. Equilibrium dissociation constant (K_D), enthalpy (ΔH), entropy (-TΔS), Gibbs free energy (ΔG) and reaction stoichiometry (n) are shown. Protein-protein interaction affinity is defined by Gibbs energy for binding: $\Delta G = -RT \ln K_A = RT \ln K_D$. ΔG has two different contributions, ΔH and -TΔS, according to equation ΔG = ΔH - TΔS. *Cooperativity parameters (Gibbs energy [Δg], enthalpy [Δh] entropy [-TΔs] and cooperativity constant [*k*]) are indicated for cooperative binding. nd, not determined.

Protein complex	10 mM sodium phosphate pH 7.4					10 mM sodium phosphate pH 7.4 + 100 mM KCl				
	ΔG (kcal mol^{-1})	**ΔH (kcal mol^{-1})**	**-TΔS (kcal mol^{-1})**	**K_D (μM)**	**n**	**ΔG (kcal mol^{-1})**	**ΔH (kcal mol^{-1})**	**-TΔS (kcal mol^{-1})**	**K_D (μM)**	**n**
Cc:SET/TAF-Iβ	-7.5 (Δg -0.8)*	-0.9 (Δh 6.1)*	-6.6 (-TΔs -6.9)*	3.1 (*k* 3.8)*	2.0	-6.5 (Δg 0.4)*	-2.8 (Δh -7.4)*	7.8 (-TΔs -3.7)*	16 (*k* 0.52)*	2.2
H2B:SET/TAF-Iβ	-7.8	-2.6	-5.2	2.0	2.1	-6.6	-20.0	13.4	13	1.8
H3:SET/TAF-Iβ	-6.3	-3.9	-2.4	25	2.0	-5.9	-18.1	12.2	50	2.0
H4:SET/TAF-Iβ	-7.1	-1.4	-5.7	6.0	1.9	-6.4	-20.3	13.9	21	1.9
Cc:SET/TAF-Iβ$_{(1-80)}$	-5.9	1.9	-7.8	44	0.98	-5.5	4.0	-9.5	90	1.1
Cc:SET/TAF-Iβ$_{(81-277)}$	-6.8	6.7	-13.5	9.6	0.98	-6.1	3.8	-9.9	31	1.2
Cc:S162A/K164A/D165A	-7.1	-2.4	-4.7	6.3	1.9	nd	nd	nd	nd	nd
Cc:T191A/T194A/D195A	-6.4	-4.4	-2.0	22	1.9	-6.0	-30.2	24.2	38	1.8